

EDGE ARTICLE

View Article Online
View Journal | View IssueCite this: *Chem. Sci.*, 2020, **11**, 6766

All publication charges for this article have been paid for by the Royal Society of Chemistry

Ruthenium-catalyzed hydrogenation of CO₂ as a route to methyl esters for use as biofuels or fine chemicals†Zheng Wang,^{abc} Ziwei Zhao,^a Yong Li,^a Yanxia Zhong,^d Qiuyue Zhang,^b Qingbin Liu,^{de} Gregory A. Solan,^{be} Yanping Ma^b and Wen-Hua Sun^{ab}

A novel robust diphosphine–ruthenium(II) complex has been developed that can efficiently catalyze both the hydrogenation of CO₂ to methanol and its *in situ* condensation with carboxylic acids to form methyl esters; a TON of up to 3260 is achievable for the CO₂ to methanol step. Both aromatic and aliphatic carboxylic acids can be transformed to their corresponding methyl esters with high conversion and selectivity (17 aliphatic and 18 aromatic examples). On the basis of a series of experiments, a mechanism has been proposed to account for the various steps involved in the catalytic pathway. More importantly, this approach provides a promising route for using CO₂ as a C1 source for the production of biofuels, fine chemicals and methanol.

Received 26th May 2020

Accepted 5th June 2020

DOI: 10.1039/d0sc02942d

rsc.li/chemical-science

Introduction

The steadily rising levels of carbon dioxide in the atmosphere over the last hundred years or so have made a major contribution to the earth's greenhouse effect. These higher concentrations can be attributed, in large measure, to increasing worldwide energy consumption that is generated through power plants that make use of fossil resources.¹ However, in order to maintain the carbon dioxide balance in the atmosphere and to reduce the dependency on a limited fossil resource, alternative ways for the sustainable production of fuels and chemicals represent a major global challenge. A strategy that has been gaining attention is the use of captured CO₂ as a feedstock for the synthesis of biofuels and chemicals.² In recent decades, chemists have explored and developed more than one hundred laboratory processes for using CO₂ as an alternative carbon source in fields that interface the chemical

and energy sectors (Scheme 1).^{1b} Such processes include the direct metal-catalyzed hydrogenation of CO₂ to formic acid,³ formides,⁴ methanol⁵ and ethanol.⁶ In addition, there has been the use of CO₂ as a C1 building block in hydroxymethylation,⁷ *N*-methylation of amines/amides,⁸ *N*-methylation of imines,⁹ methylation of C–H bonds (sp³)¹⁰ as well as the carboxylation of C–H (sp²)¹¹ and N–H bonds.¹² Elsewhere, the non-reductive incorporation of a CO₂ molecule into organic products, such as cyclic carbonates and polycarbonates/polyethercarbonates has been demonstrated.^{1a,1b,13}

From an industrial standpoint, relatively few processes employ CO₂ as a starting material for the manufacture of organic products.^{2,13e} Nevertheless, those processes that do operate allow access to a number of high demand materials including urea, methanol, salicylic acid, organic carbonates and polycarbonates.^{1a,1b,13} Staggeringly however, this use of CO₂ as a feedstock for chemicals only accounts for about 0.36% of

^aHebei Key Laboratory of Organic Functional Molecules, College of Chemistry and Material Science, Hebei Normal University, Shijiazhuang 050024, China. E-mail: liuqingb@sina.com

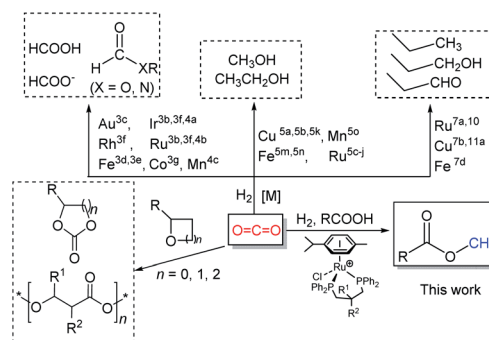
^bKey Laboratory of Engineering Plastics and Beijing National Laboratory for Molecular Science, Institute of Chemistry, Chinese Academy of Sciences, Beijing 100190, China. E-mail: gas8@leicester.ac.uk; whsun@iccas.ac.cn; Fax: +86-10-62618239; Tel: +86-10-62557955

^cCollege of Science, Agricultural University of Hebei, Baoding 071001, China

^dDepartment of Nursing Shijiazhuang Medical College, Shijiazhuang 050000, China

^eDepartment of Chemistry, University of Leicester, University Road, Leicester LE1 7RH, UK

† Electronic supplementary information (ESI) available: Detailed experimental procedures, spectra (NMR, GC-MS, LC-MS), Fig. S1–S19, Tables S1–S6. CCDC 1961855 (Ru2) and 1961856 (Ru3). For ESI and crystallographic data in CIF or other electronic format see DOI: 10.1039/d0sc02942d



Scheme 1 Capturing CO₂ as a carbon source for the production of fine chemicals and biofuels.

global CO₂ emissions.¹⁴ Elsewhere, it has been stated that only by completely using biomass energy (and without fossil energy), can the concentration of carbon dioxide reach equilibrium in the atmosphere.¹⁴ Moreover, it could be argued that one of the best ways to reduce CO₂ emissions would be to synthesize biofuels that could be recycled.

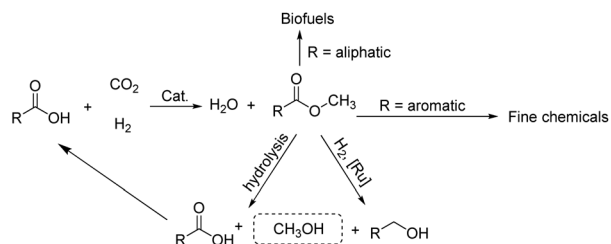
As part of an ongoing program, we have been interested in developing methods of using CO₂ as a feedstock to form carboxylic acid methyl esters as their aliphatic examples could then be used as biofuels while their aromatic methyl esters as fine chemicals (Scheme 2). In particular, a cascade strategy involving metal-catalyzed hydrogenation of CO₂ to methanol and then *in situ* condensation of methanol with a carboxylic acid has been envisioned. Of course, the carboxylic acids represent attractive family of reactants as they can in principle be obtained from biomass. Furthermore, the catalytic hydrogenation of methyl esters has been shown by us¹⁵ and others,^{5c–5e,16} to give alkyl/aryl alcohols and methanol which can, in their own right, serve as important fuels and synthetic building blocks.^{15,16} Alternatively, methanol can be produced by the hydrolysis of a methyl ester and the corresponding carboxylic acid by-product recycled. Overall, this sequence of reactions could present an elegant and green sustainable route for the production of fuels and chemicals.

To realize our goal, we herein disclose a new family of well-defined diphosphine–ruthenium(II) cationic complexes that can serve as versatile (pre)catalysts for the conversion of CO₂ to a raft of different types of methyl ester (Scheme 1). By performing the reactions in the presence of a carboxylic acid, we show that this acid plays two key roles; (i) as a reactant in the conversion of the methanol intermediate to the target methyl ester and (ii) as a promoter in the CO₂ hydrogenation step. Unlike the ruthenium–triphos catalysts previously reported by Leitner and others for the hydrogenation of CO₂,^{5c,5f} the current (pre)catalysts are based on an organometallic η⁶-arene–ruthenium core that incorporates a chelating diphosphine of the type, CR¹R²(CH₂PPh₂)₂ [R¹ = CH₂-PPh₂, R² = Me; R¹ = CH₂P(O)Ph₂, R² = Me; R¹ = CH₂P(O)Ph₂, R² = Et; R¹ = R² = H].

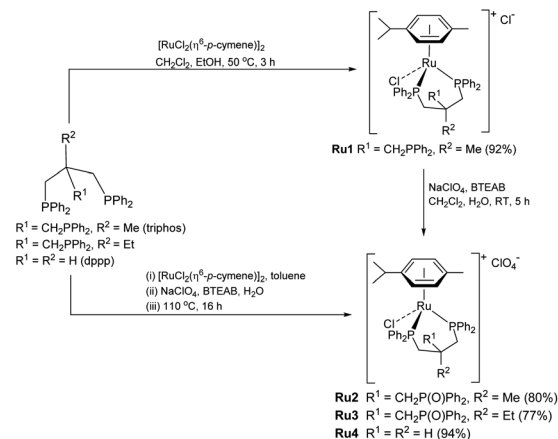
Results and discussion

Synthesis and characterization of Ru1–Ru4

Cationic [RuCl(κP,κP-triphos)(η⁶-p-cymene)][Cl] (**Ru1**) was prepared in excellent yield by the reaction of [RuCl₂(η⁶-p-cymene)]₂ with 1,1,1-tris(diphenylphosphinomethyl)ethane



Scheme 2 Potential strategy involving CO₂ utilization to form industrially useful methyl esters and their amenability to recycling and use in other applications.



Scheme 3 Synthetic route to Ru1–Ru4.

(triphos) in a mixture of CH₂Cl₂ and EtOH at 50 °C (Scheme 3, see ESI†); related ruthenium(II) complexes and reaction conditions have been reported elsewhere.¹⁷ The ³¹P NMR spectrum of **Ru1** exhibited two singlet peaks at δ 26.02 and δ 24.81, corresponding to the inequivalent phosphine donors, as well as one single peak at δ –29.77 for the pendant phosphine (see ESI, Fig. S3†).

Counteranion exchange and oxidation of the pendant phosphine arm in **Ru1** and could be readily achieved by its reaction with sodium perchlorate in a mixture of dichloromethane and water at room temperature to give [RuCl(κP,κP-triphos(O))(η⁶-p-cymene)][ClO₄] (**Ru2**) (Scheme 3). Alternatively, **Ru2** could be obtained by a one-pot reaction involving successive treatment of triphos with [RuCl₂(η⁶-p-cymene)]₂ and sodium perchlorate in a water/toluene mixture; benzyltriethylammonium bromide (BTEAB) was used as a phase transfer catalyst in both routes. The ³¹P NMR spectrum of **Ru2** in DMSO-*d*₆ exhibited two mutually coupled doublets at δ 26.18 and δ 25.05, which were assigned to the signals for the

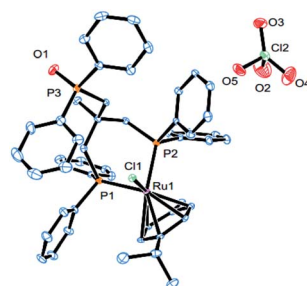


Fig. 1 ORTEP representation of **Ru2**. Thermal ellipsoids are shown at the 30% probability level; hydrogen atoms have been omitted for clarity. Selected bond distances (Å): Ru1–Cl1 = 2.4086(11), Ru1–P2 = 2.3276(12), Ru1–P1 = 2.3286(12), Ru1–C47 = 2.221(4), Ru1–C46 = 2.269(4), Ru1–C45 = 2.322(4), Ru1–C43 = 2.254(4), Ru1–C44 = 2.260(4), Ru1–C48 = 2.295(5), P3–O1 = 1.480(3); Selected angles (deg): P1–Ru1–Cl1 = 85.07(3), P2–Ru1–Cl1 = 87.77(4), P2–Ru1–P1 = 86.85(2).

inequivalent phosphine donors; a single peak at δ 28.32 was attributed to the non-coordinated phosphine oxide (see ESI, Fig. S9†).

Complex cations $[\text{RuCl}\{\kappa P, \kappa P-(\text{CH}_2\text{PPh}_2)_2\text{CR}^1\text{R}^2\}(\eta^6\text{-}p\text{-cymene})][\text{ClO}_4]$ [**Ru3** $\text{R}^1 = \text{CH}_2\text{P}(\text{O})\text{Ph}_2$, $\text{R}^2 = \text{Et}$; **Ru4** $\text{R}^1 = \text{R}^2 = \text{H}$] could be obtained from $\text{CEt}(\text{CH}_2\text{PPh}_2)_3$ or $\text{CH}_2(\text{CH}_2\text{PPh}_2)_2$ (dppp), respectively, in high yield by using a one-pot route based on that employed for the synthesis of **Ru2**. As with **Ru2**, **Ru3** showed two doublets in the ^{31}P NMR spectrum for the inequivalent coordinated phosphines and a singlet for the pendant phosphine oxide group, while **Ru4** showed two distinct singlets for the bidentate dppp ligand. Besides ^{31}P NMR spectroscopy, all four ruthenium complexes were characterized by ^1H , ^{13}C NMR spectroscopy, elemental analysis and by ESI-mass spectrometry (Table S3, see ESI†). To confirm their structural identity, **Ru2** and **Ru3** were the subject of single crystal X-ray diffraction studies (Fig. 1 and 2); selected bond distances and angles are given in the figure captions. Both structures consist of a cationic ruthenium(II) unit and a non-coordinating perchlorate anion. The cationic unit adopts a three-legged piano stool geometry comprising a $\eta^6\text{-}p\text{-cymene}$, a monodentate chloride and a bidentate $\text{CR}^2(\text{CH}_2\text{-P}(\text{O})\text{Ph}_2)(\text{CH}_2\text{PPh}_2)_2$ ($\text{R}^2 = \text{Me}$ **Ru2**, Et **Ru3**) ligand which binds through the diphenylphosphine phosphorus atoms while the oxidized phosphine arm remains uncoordinated; the bond parameters around ruthenium are not exceptional and indeed similar to related half-sandwich structures. To try and explain the origin of the phosphine oxide units in **Ru2** and **Ru3**, the four different ruthenium complexes were separately evaluated as catalysts for the oxidation of PPh_3 in a toluene–water mixture at 100°C over 24 hours (Table S2, ESI†). Inspection of the results revealed conversions to triphenylphosphine oxide of 24% for $[\text{RuCl}_2(\eta^6\text{-}p\text{-cymene})_2]$, 94% for **Ru1**, 43% for **Ru2** and 97% for $[[\text{RuCl}_2(\eta^6\text{-}p\text{-cymene})_2] + \text{triphos}]$. Evidently, the uncoordinated phosphine oxide present in **Ru2** and **Ru3** derives from a ruthenium-mediated oxidation of the corresponding $-\text{CH}_2\text{PPh}_2$ unit.

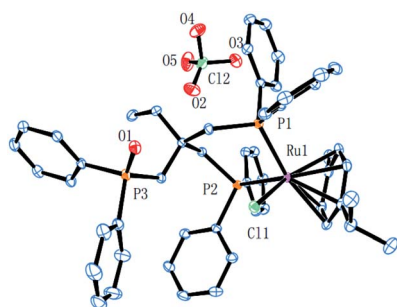


Fig. 2 ORTEP representation of **Ru3**. Thermal ellipsoids are shown at the 30% probability level; hydrogen atoms have been omitted for clarity. Selected bond distances (Å): Ru1–Cl1 = 2.4249(7), Ru1–P1 = 2.3333(7), Ru1–P2 = 2.3193(6), Ru1–C43 = 2.322(2), Ru1–C44 = 2.285(2), Ru1–C45 = 2.224(2), Ru1–C46 = 2.298(2), Ru1–C47 = 2.241(2), Ru1–C48 = 2.248(2), P3–O1 = 1.4893(15); Selected angles (deg $^\circ$): P1–Ru1–Cl1 = 82.55(3), P2–Ru1–Cl1 = 90.39(3), P2–Ru1–P1 = 86.76(2).

Catalytic hydrogenation of CO_2 to give carboxylic acid methyl esters

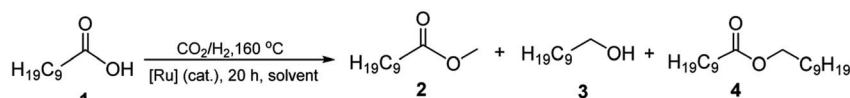
(a) Optimization of conditions. To allow an optimization of the conditions, **Ru2** was selected as the (pre)catalyst and decanoic acid (**1**) as the carboxylic acid substrate with 30 mL of 1,2-dimethoxyethane (DME) as solvent (Table 1). With the reaction temperature set at 160°C , the combined pressure of CO_2 and H_2 at 80 bar (12 : 68 ratio) and the substrate to catalyst molar ratio (S : C) at 100 : 1, a 28% conversion was observed after 20 hours of which 25% constituted methyl decanoate (**2**) and 3% *n*-decanol (**3**) (entry 1, Table 1). By slightly increasing the hydrogen pressure in the gaseous mixture to 12 : 70, the conversion decreased to 14% with a larger proportion now being **3** (entry 2, Table 1). Under the same conditions but with the volume of solvent reduced to 10 mL, to increase the substrate concentration, a 91% conversion was achieved with 83% being **2** (entry 3, Table 1). To our delight, by reverting to the pressure ratio of CO_2 : H_2 = 12 : 68 and maintaining the higher concentration of substrate, a high conversion and selectivity (conv. = 99%, selectivity = 100%) were realized (entry 4, Table 1).

With a view to establishing the most compatible reaction medium for the hydrogenation using **Ru2**, four related solvents were screened, namely, DME, 1,2-diethoxyethane, diglyme and triglyme (entries 4–7, Table 1). On examination of the data, DME was the standout performer in terms of the conversion (99%) and selectivity for **2** (100%). When 1,2-diethoxyethane was employed as solvent, a lower conversion (76%) and selectivity (92%) was observed while with the longer chain solvents, diglyme and triglyme, the conversions observed were markedly less at 36% and 65%, respectively.

In order to determine the optimal S : C ratio, four different combinations, 100 : 1, 200 : 1, 500 : 1 and 1000 : 1, were screened using **Ru2** (entries 4 and 8–10, Table 1). It was found that with ratios between 100 : 1 and 500 : 1, high conversions (96–100%) could be achieved. By contrast with the ratio at 1000 : 1, the CO_2 hydrogenation was incomplete with only 42% conversion achievable (entry 10, Table 1). With the volume of DME decreased to 2.5 mL and a 100 : 1 ratio re-deployed, 100% conversion was obtained, but the ester products consisted of **2** (95%) and ethyl decanoate (5%) (entry 11, Table 1, see ESI†). By contrast, when $[\text{RuCl}_2(p\text{-cymene})_2]$ was employed as catalyst, no methyl decanoate was obtained instead minor amounts of **3** and decyl decanoate (**4**) were detected (entry 12, Table 1). In addition, when the catalysis was conducted using **Ru2** but in the absence of decanoic acid, no CH_3OH was observed (entry 17, Table 1), which suggests that the decanoic acid acts as a promoter.

Using the best overall set of conditions established for **Ru2** [$T = 160^\circ\text{C}$, CO_2/H_2 = 12 : 68 (80 bar in total), S : C = 100 : 1, 20 h, DME (10 mL)], the remaining ruthenium complexes **Ru1**, **Ru3** and **Ru4** were also evaluated. Indeed, all of these complexes were active and selective catalysts for methyl decanoate with their conversions, when compared to **Ru2**, falling in the order: **Ru2** > **Ru1** > **Ru3** > **Ru4** (entries 4, 13–15, Table 1). As a control, no conversion to **2** was achieved when the hydrogenation was performed in the absence of CO_2 under the same conditions (entry 16, Table 1).



Table 1 Catalytic evaluation of the hydrogenation of CO₂ in the presence of decanoic acid (1), to give methyl decanoate (2)^a

Entry	S : C	[Ru]	Solvent	CO ₂ : H ₂ (bar)	Conv. ^b (%)	2/3/4 ^b (% conv. to each)
1 ^c	100 : 1	Ru2	DME	12 : 68	28	25/3/0
2 ^c	100 : 1	Ru2	DME	12 : 70	14	12/2/0
3	100 : 1	Ru2	DME	12 : 70	91	83/8/0
4	100 : 1	Ru2	DME	12 : 68	99	99/0/0
5	100 : 1	Ru2	1,2-Diethoxyethane	12 : 68	76	70/6/0
6	100 : 1	Ru2	Diglyme	12 : 68	36	30/6/0
7	100 : 1	Ru2	Triglyme	12/68	65	60/5/0
8	200 : 1	Ru2	DME	12 : 68	96	94/2/0
9	500 : 1	Ru2	DME	12 : 68	100	100/0/0
10	1000 : 1	Ru2	DME	12 : 68	42	40/2/0
11 ^d	100 : 1	Ru2	DME	12 : 68	100	100/0/0
12	100 : 1	[RuCl ₂ (<i>p</i> -cymene)] ₂	DME	12 : 68	3	0/2/1
13	100 : 1	Ru1	DME	12 : 68	76	76/0/0
14	100 : 1	Ru3	DME	12 : 68	67	67/0/0
15	100 : 1	Ru4	DME	12 : 68	56	56/0/0
16 ^e	100 : 1	Ru2	DME	00 : 80	n.d.	n.d.
17 ^f	100 : 1	Ru2	DME	12 : 68	n.d.	n.d.

^a Conditions: decanoic acid (1.0 mmol), [Ru] (1.0–10.0 μmol), solvent (10 mL), P_{H_2} = 68–70 bar (at RT), P_{CO_2} = 0–12 bar (at RT), temp. = 160 °C, time = 20 h, S : C = the molar substrate to catalyst ratio, DME is 1,2-dimethoxyethane. ^b The conversion, with reference to decanoic acid (1), was determined by GC (using mesitylene as the internal standard) and by GC-MS. ^c 30 mL of DME in place of 10 mL. ^d DME (2.5 mL), the ester products are methyl decanoate (95%) and ethyl decanoate (5%). ^e In the absence of CO₂. ^f In the absence of decanoic acid (1), no CH₃OH was observed.

(b) Exploring the substrate scope of Ru2. With the aim to explore the scope and functional group tolerance of **Ru2** as a catalyst for the hydrogenation of CO₂ to methyl esters, a broad range of aliphatic carboxylic acids was investigated as substrates. The effects of carbon chain length of both mono- and dicarboxylic acids as well as unsaturation within the aliphatic chain were all factors to be evaluated using the optimal conditions established using decanoic acid. In addition, the effect of using decanoic acid as an additive was also investigated. The complete set of results are listed in Table 2.

For aliphatic carboxylic acids containing carbon chain lengths of $C \leq 5$, low conversions and low selectivity were evident after a 20 hour run time. For example, only 10% of methyl acetate was observed when using acetic acid and 6% of methyl pentanoate when using pentanoic acid (entries 1 and 2, Table 2). By contrast, the longer chain lengths ($6 \leq C \leq 10$) showed excellent conversions and high selectivity for the corresponding methyl ester (entries 3–7, Table 2). In the case of hexanoic acid, it was shown that in the absence of solvent the selectivity dramatically reduced [100% (with DME) to 54% (without), entries 3 and 4, Table 2] producing 54% methyl hexanoate, 12% of hexyl hexanoate and 33% 1-hexanol (entry 4, Table 2).

Intriguingly, decanoic acid (1) can also be used as additive for adjusting the activity and selectivity of the ruthenium catalyst. For example, using undecanoic acid as the substrate, the selectivity for the methyl ester increased from 81% to 100% and the conversion from 96% to 99% when 10 mol% decanoic acid

was introduced (entries 8 vs. 9, Table 2). The longer carbon chain aliphatic acids ($12 \leq C \leq 19$) also gave excellent results in the presence of decanoic acid as an additive (entries 10–13, Table 2). Significantly, many of the resulting aliphatic esters are in the range of biodiesels.¹⁸

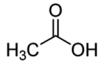
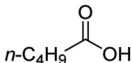
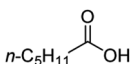
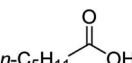
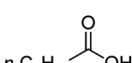
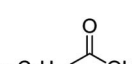
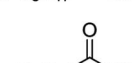
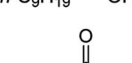
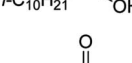
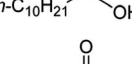
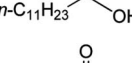
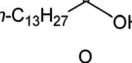
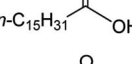
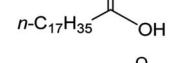
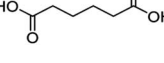
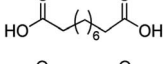
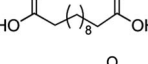
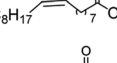
For dicarboxylic acids incorporating aliphatic linkers of a range of chain lengths, all underwent 99% conversion with 95–100% selectivity. However, it was noted that longer reaction times (up to 24 hours) were needed to complete the transformation when compared to those containing only one carboxyl group (entries 14–16, Table 2). It was also apparent that the shorter carbon chain dicarboxylic acid, adipic acid, was at the lower end of the selectivity (95%) range with 94% dimethyl adipate and 5% of 6-methoxy-6-oxohexanoic acid produced (entry 14, Table 2).

In the case of aliphatic carboxylic acids incorporating some unsaturation, methyl ester formation was also achievable but at the expense of double bond (C=C) hydrogenation. For example, 99% of methyl benzenepropanoate was obtained when using cinnamic acid while 98% of methyl octadecanoate were observed from octadec-9-enoic acid (entries 17 and 18, Table 2).

The hydrogenation capacity of **Ru2** is not limited to aliphatic carboxylic acids. Indeed, a wide variety of aromatic examples differing in their *ortho*-, *meta*- and *para*-substitution patterns, also showed excellent conversions and selectivity for methyl esters (**6a–6r**) (Table 3). For example, benzoic acid (**5a**) underwent 93% conversion to methyl benzoate (**6a**) with a S : C ratio of 100 : 1 that only reduced to 69% (99% selectivity) when the



Table 2 Hydrogenation of carbon dioxide to aliphatic esters^a

$\text{alkyl}-\text{C}(=\text{O})\text{OH} \xrightarrow[\text{DME, 160 } ^\circ\text{C, 20 - 24 h}]{\text{Ru2 (cat.), CO}_2/\text{H}_2} \text{alkyl}-\text{C}(=\text{O})\text{OCH}_3$					
Entry	Substrate	S : C	<i>t</i> (h)	Conv. ^b (%)	Ester/alcohol ^b (% conv. to each)
1		100 : 1	20	16	10/6
2		100 : 1	20	10	6/4
3		500 : 1	20	100	100/0
4 ^c		500 : 1	20	99	66(54/12)/33
5		500 : 1	20	100	100/0
6		500 : 1	20	99	99/0
7		500 : 1	20	100	100/0
8		500 : 1	20	96	78/18
9 ^d		500 : 1	20	99	99/0
10 ^d		500 : 1	20	99	99/0
11 ^d		500 : 1	20	99	99/0
12 ^d		100 : 1	20	99	99/0
13 ^d		100 : 1	20	99	99/0
14 ^e		500 : 1	24	99	94/5
15		500 : 1	24	99	99/0
16		500 : 1	24	99	99/0
17 ^{d,f}		500 : 1	20	98	98/0
18 ^g		500 : 1	20	99	99/0

^a Reaction conditions: substrate (1.0 mmol), **Ru2** (2.0–10.0 μmol), DME (10 mL), P_{H_2} = 68 bar (at RT), P_{CO_2} = 12 bar (at RT), temp. = 160 °C, S : C = the molar substrate to catalyst ratio. ^b The conversion with reference to the carboxylic acid was determined by GC (using mesitylene as the internal standard) and by GC-MS. ^c In the absence of solvent; 54% of methyl hexanoate and 12% of heptyl hexanoate were produced. ^d In the presence of decanoic acid (0.1 mmol) as additive. ^e 5% of the product is 6-methoxy-6-oxohexanoic acid. ^f The product is methyl stearate. ^g The product is methyl benzenepropanoate.



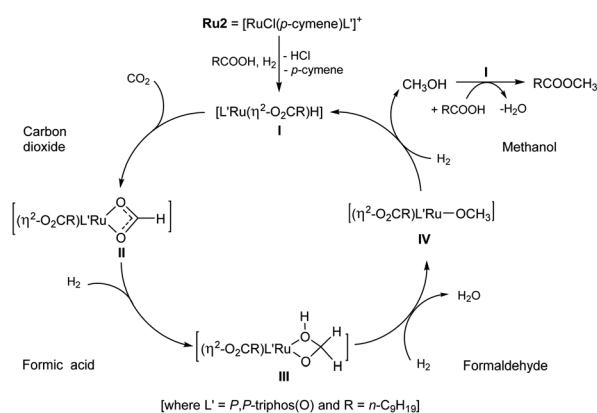
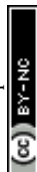
Table 3 Conversion of aryl carboxylic acids (**5**) to aromatic methyl esters (**6**) via the Ru-mediated hydrogenation of carbon dioxide^a

$\text{aryl-COOH} \xrightarrow[\text{DME, 160 } ^\circ\text{C, 20 h}]{\text{Ru2 (cat.), CO}_2/\text{H}_2} \text{aryl-COOCH}_3$			
Substrate	Product ^b (conv.%)	Substrate	Product ^b (conv.%)
5a R = H	6a R = H, 93%, 6a 69% ^c	5f R = F	6f R = F, 99%
5b R = F	6b R = F, 99%	5g R = Cl ^d	6a 99%
5c R = Cl ^d	6a 99%	5h R = Br ^d	6a 99%
5d R = Br ^d	6a 99%	5i R = CF ₃	6i R = CF ₃ , 99%
5e R = CF ₃	6e R = CF ₃ , 99%		
		5o	6o 82%
5j R = F	6j R = F, 78%		
5k R = Cl ^d	6a 99%	5p	6o' 18%
5l R = Br ^d	6a 99%		
5m R = CF ₃	6m R = CF ₃ , 73%	5r	6p 99%
5n R = Me	6n R = Me, 100%		
		5q	6r 65%
			6r' 35%

^a Conditions: substrate (1.0 mmol), **Ru2** (10.0 μmol), S : C = 100 : 1, DME (10 mL), P_{H_2} = 68 bar (at RT), P_{CO_2} = 12 bar (at RT), temp. = 160 °C, time = 20 h. ^b The conversion, with reference to the carboxylic acid, was determined by GC (using mesitylene as the internal standard) and by GC-MS. ^c **Ru2** (2.0 μmol), S : C = 500 : 1. ^d A dehalogenation reaction occurs with the product being methyl benzoate (**6a**).

ratio was increased to 500 : 1. Interestingly, benzoic acids (**5b–5e**, **5f–5h**, **5j–5l**) incorporating electron withdrawing groups such as halides (F, Cl, Br) or CF₃ at the *ortho*- (**5b–5e**), *meta*- (**5f–5h**) or *para*-positions (**5j–5l**) showed little variation in conversion (73–99%) and selectivity (almost 100%) for the methyl ester. However, dehalogenation was an outcome of all benzoic acids containing either Cl or Br substituents resulting in methyl benzoate as the sole methyl ester product in these cases (see substrates **5c**, **5d**, **5g**, **5h**, **5k**, **5l**); this finding can likely be attributed to the high temperature and the reactivity of **Ru2** towards the C_{aryl}–X bonds present in these particular substrates. In comparison, the electron-rich benzoic acids with methyl or methoxy substituents (**5n** and **5o**) at the *para*-positions gave 100% conversions to their methyl esters (**6n** and **6o**). Interestingly, *p*-methoxybenzoic acid (**5o**) produced two kinds of esters, methyl 4-methoxybenzoate (**6o**, 82%) and ethyl 4-methoxybenzoate (**6o'**, 18%). The presence of **6o'** would suggest that the hydrogenation of CO₂ produced a small amount of the higher alcohol ethanol which then underwent condensation with *p*-methoxybenzoic acid (**5o**) to give **6o'**; the mechanism of ethanol production from CO₂ is assumed to be similar to that reported by Han.⁶ Furan-2-carboxylic acid (**5p**) also resulted in 99% conversion and 100% selectivity (**6p**). Notably, the difluoro-substitution on the aryl ring did not affect the reaction with 3,4-difluorobenzoic acid (**5q**) also producing 99% of methyl 3,4-

difluorobenzoate (**6q**). In addition, the dicarboxyl-substituted isophthalic acid (**5r**), though reaching 100% conversion, displayed a slight difference in reactivity when compared to benzoic acid by producing 65% of the dimethylester (**6r**) and 35% of the methyl ethyl ester (**6r'**). Once again the hydrogenation of CO₂ to form a small amount of ethanol seems likely to account for the formation of **6r'**.

**Scheme 4** Proposed mechanism for the **Ru2** catalyzed hydrogenation of CO₂ to methyl decanoate in the presence of decanoic acid via Ru(II) intermediates derived from formic acid, formaldehyde and methanol.

(c) Mechanistic pathway. Based on the recent work concerning the ruthenium-catalyzed hydrogenation of CO₂ to methanol,^{3,5f,5k,19} an acid additive can act as promoter in a carboxylate assisted proton transfer.^{5f} Hence, a plausible catalytic cycle is shown in Scheme 4 involving Ru(II) intermediates derived from formic acid, formaldehyde and methanol. Firstly, the neutral carboxylate complex, [L'Ru(η²-O²CR)H] (**I**, L' = κP,κP-triphos(O)), is formed through the heterolytic cleavage of hydrogen and substitution of *p*-cymene for decanoate. Despite multiple attempts, crystallization of **I** proved unsuccessful. Nonetheless, several examples of penta-coordinate intermediates similar to **I** have been reported based on the interaction of a precatalyst with a carboxylic acid.^{5f,19e} Moreover, examination of the solid species formed following work-up of the catalytic run by ¹H NMR spectroscopy showed no evidence for an η⁶-coordinated *para*-cymene (see Fig. S18, ESI†). In the next step of the catalytic cycle, CO₂ insertion can occur to give formate **II**, which is then reduced to the hydroxymethanolate species **III**. Hydrogenation of **III** and concomitant loss of water gives methoxide **IV** which can then eliminate methanol and regenerate **I** following hydrogenolysis. The methanol produced during conversion of **IV** to **I** can then undergo a ruthenium-catalyzed condensation with the carboxylic acid (decanoic acid) to form the methyl ester (methyl decanoate) and water. Notwithstanding the pathway outlined above, we cannot fully rule out the role, at some level, of ruthenium nanoparticulate species in the catalysis. However, it should be pointed out only signals corresponding to unidentified Ru-phosphine species could be detected *post-operando* in the ³¹P NMR spectrum (see Fig. S19, ESI†).

In attempt to shed some light on this proposed mechanism, the following set of experiments were conducted. Firstly, ¹H NMR spectroscopy was used to detect for methanol in the catalytic system. Using the optimal operating conditions established in entry 4 (Table 1), free methanol was indeed detected by ¹H NMR spectroscopy after 20 hours (Fig. S16, see ESI†). Furthermore, when the volume of DME was decreased from 10 mL to 2.5 mL a small amount of ethanol was also observed. This finding can explain the formation of methyl decanoate (95%) and ethyl decanoate (5%) that was observed in entry 11 (Table 1).⁶ On the other hand, there was no methanol observed when the hydrogenation was conducted in the absence of CO₂ (entry 16, Table 1, see ESI†). More importantly, in the absence of decanoic acid, no CH₃OH was observed (entry 17, Table 1), which would imply decanoic acid acts as a promoter.

Secondly, for each ruthenium catalyst (**Ru1–Ru4**), the amount of methanol produced during the hydrogenation of CO₂ when in the presence of decanoic acid (1 mmol), was quantitatively determined: conditions, 10 mL of DME at 160 °C with P_{CO₂} = 12 bar (at RT) and P_{H₂} = 68 bar (at RT) (Table 4, ESI 6.2†). To our surprise, the turnover number (TON) of **Ru2** for the direct transformation of CO₂ to methanol was up to 3262 which noticeably exceeds that previously reported by Leitner *et al.* (TON = 442, 2-MTHF as solvent, at 140 °C with P_{CO₂} = 20 bar (at RT) and P_{H₂} = 60 bar (at RT)).^{5e,5f} Although the origin of this increase remains uncertain, it does support the assertion that decanoic acid present in the catalytic system can act as a promoter in the conversion of CO₂ to methanol. It was also found that the amount of methanol produced using **Ru2** and **Ru4** proved consistent with the

Table 4 The amount of methanol produced by **Ru1–Ru4**^a

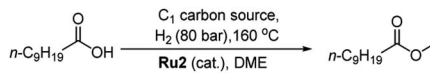
Entry	[Ru]	Conv. ^b (%)	Conv. ^c (mg mL ⁻¹)	MeOH ^d (n mmol)	TON _{MeOH} ^e
1	Ru1	76	90.03	28.12	2812
2	Ru2	99	104.4	32.62	3262
3	Ru3	67	99.31	30.94	3094
4	Ru4	56	62.36	19.49	1949

^a Conditions: decanoic acid (1.0 mmol), [Ru] (10.0 μmol), DME (10 mL), P_{CO₂} = 12 bar (at RT), P_{H₂} = 68 bar (at RT), time = 20 hours, temp. = 160 °C, S : C = 100 : 1. ^b The conversion with reference to decanoic acid was determined by GC (using mesitylene as the internal standard) and by GC-MS. ^c The conversion to methanol was determined by GC (using a standard concentration curve of methanol as the external standard (see ESI 6.2)). ^d The total volume of the reaction solution was 10 mL. ^e TON is the ratio of the moles of methanol (*n*) to the moles of catalyst (10 μmol).

percentage conversions to the methyl decanoate. On the other hand, that observed for catalysts **Ru1** and **Ru3** showed some discrepancy (entries 1 and 3, Table 4), which may be due to the structural differences of the ligands leading to the different activities for catalytic esterification.

Finally, we set about attempting to confirm that the catalytic mechanism proceeded *via* three steps involving intermediates derived from formic acid, formaldehyde and methanol.^{3h,5f,5k,19} Hence, we used MeOH, HCHO (37% wt aqueous solution) and HCOOH independently as the C1 sources in the absence of CO₂ under the same conditions. In all cases methyl decanoate was smoothly formed. However, the different carbon sources required different run times to complete the transformation (Table 5, ESI 6.1†). For example, the use of one or fifty equivalents of methanol needed less time (2–4 hours) to be converted to methyl decanoate than that using formaldehyde and formic acid. Indeed, using formic acid took close to 20 hours to allow a comparable conversion. Although uncertain at this stage, it would seem likely that the rate-determining step in the catalytic

Table 5 Using MeOH, HCHO, HCOOH as the C1 carbon source for the production of methyl decanoate^a

					
Entry	C1 carbon source	S : C	<i>t</i> (h)	Conv. ^b (%)	Ester/alcohol ^b (yield%)
1	MeOH (50 eq.)	100 : 1	2	99	99/0
2	MeOH (1 eq.)	100 : 1	4	99	99/0
3	HCHO ^c (1 eq.)	100 : 1	10	99	99/0
4	HCO ₂ H (1 eq.)	100 : 1	20	99	99/0
5	MeOH (1 eq.)	100 : 0	4	5	5/0

^a Reaction conditions: decanoic acid (1 mmol), **Ru2** (10 μmol), DME (10 mL), P_{H₂} = 80 bar (at RT), temp. = 160 °C, S : C = the molar substrate to catalyst ratio. ^b The conversion with reference to the decanoic acid was determined by GC (using mesitylene as the internal standard) and by GC-MS. ^c 37% wt aqueous solution.



cycle is located in the sequence of steps leading from HCOOH to CH₃OH.^{3h,5j,5k,19} As a final point, only 5% conversion to methyl decanoate was observed in the absence of **Ru2** (entry 4, Table 5).

Conclusions

We have developed a novel route to prepare a wide range of methyl esters from CO₂ via a ruthenium catalyzed hydrogenation to methanol and *in situ* condensation with a carboxylic acid. By evaluating four structurally related diphosphine-ruthenium (pre)catalysts, complex [RuCl(κP,κP-triphos(O))(η⁶-p-cymene)](ClO₄) (**Ru2**) has shown the greatest efficiency for the transformation. Indeed using **Ru2**, both aromatic and aliphatic carboxylic acids can be converted with high selectivity to the corresponding carboxylic acid methyl ester. Furthermore, we have also probed the mechanism through a series of experiments, which has shown that the pathway involves the direct hydrogenation of CO₂ to form consecutively formic acid, formaldehyde and methanol which then finally undergoes condensation with carboxylic acids to form the corresponding methyl ester. Moreover, this work also presents an original and effective ruthenium catalyzed process for producing methanol from CO₂ with the TON for the CO₂ to methanol step up to 3262; the role of the carboxylic acid as a promoter in this reaction has been demonstrated. More importantly, this work provides an attractive route for the utilization of CO₂ as a carbon source for the production of biofuels and fine chemicals. We therefore hope that this report will inspire the development of more efficient metal-catalyzed hydrogenation reactions of CO₂ and ultimately reduce the demand for fossil resources.

Experimental section

Catalytic study

Under an atmosphere of argon, a stainless steel 100 mL autoclave, equipped with a magnetic stir bar, was charged with **Ru1–Ru4** (2.5–10 μmol) and the solvent to be used (2.5–5 mL). A solution of the carboxylic acid (1 mmol) in the solvent (5–25 mL) was then added *via* a syringe. The autoclave was purged by three cycles of pressurization/venting with CO₂ (5–10 bar), and then pressurized with the desired mixture of CO₂ and H₂. The autoclave was heated to the desired temperature and the contents stirred. After the pre-determined reaction time, the autoclave was cooled to room temperature and the pressure slowly released. The reaction mixture was filtered through a plug of silica gel and then analyzed by GC and GC-MS.

Conflicts of interest

There are no conflicts to declare.

Acknowledgements

We acknowledge the support from the National Natural Science Foundation of China (21871275), the Nature Science Foundation of Hebei Province (B2019205149) and Talent Introduction Foundation of Agricultural University of Hebei (YJ201931). GAS

thanks the Chinese Academy of Sciences for a President's International Fellowship for visiting scientists.

Notes and references

- (a) M. Aresta, A. Dibenedetto and A. Angelini, *Chem. Rev.*, 2014, **114**, 1709–1742; (b) J. Klankermayer, S. Wesselbaum, K. Beydoun and W. Leitner, *Angew. Chem., Int. Ed.*, 2016, **55**, 7296–7343; (c) J. M. Thomas and K. D. M. Harris, *Energy Environ. Sci.*, 2016, **9**, 687–708.
- (a) P. Markewitz, W. Kuckshinrichs, W. Leitner, J. Linssen, P. Zapp, R. Bongartz, A. Schreiber and T. E. Müller, *Energy Environ. Sci.*, 2012, **5**, 7281–7305; (b) Q.-W. Song, Z.-H. Zhou and L.-N. He, *Green Chem.*, 2017, **19**, 3707–3728; (c) W. H. Wang, Y. Himeda, J. T. Muckerman, G. F. Manbeck and E. Fujita, *Chem. Rev.*, 2015, **115**, 12936–12973; (d) N. Assen, L. J. Muller, A. Steingrube, P. Voll and A. Bardow, *Energy Environ. Sci.*, 2016, **50**, 1093–1101; (e) K. Sordakis, C. Tang, L. K. Vogt, H. Junge, P. J. Dyson, M. Beller and G. Laurenczy, *Chem. Rev.*, 2018, **118**, 372–433; (f) J. Artz, T. E. Muller, K. Thenert, J. Kleinekorte, R. Meys, A. Sternberg, A. Bardow and W. Leitner, *Chem. Rev.*, 2018, **118**, 434–504; (g) S. Kar, A. Goepfert and G. K. S. Prakash, *Acc. Chem. Res.*, 2019, **52**, 2892–2903; (h) J. R. Cabrero-Antonino, R. Adam and M. Beller, *Angew. Chem., Int. Ed.*, 2019, **58**, 2–21; (i) W. Zhou, K. Cheng, J. Kang, C. Zhou, V. Subramanian, Q. Zhang and Y. Wang, *Chem. Soc. Rev.*, 2019, **48**, 3193–3228; (j) S. Wang and C. Xi, *Chem. Soc. Rev.*, 2019, **48**, 382–404.
- Select recent examples for forming formic acid: (a) P. G. Jessop, T. Ikariya and R. Noyori, *Nature*, 1994, **368**, 231–233; (b) R. Tanaka, M. Yamashita and K. Nozaki, *J. Am. Chem. Soc.*, 2009, **131**, 14168–14169; (c) D. Preti, C. Resta, S. Squarciarupi and G. Fachinetti, *Angew. Chem., Int. Ed.*, 2011, **50**, 12551–12554; (d) C. Ziebart, C. Federsel, P. Anbarasan, R. Jackstell, W. Baumann, A. Spannenberg and M. Beller, *J. Am. Chem. Soc.*, 2012, **134**, 20701–20704; (e) R. Langer, Y. Diskin-Posner, G. Leitius, L. J. W. Shimon, Y. Ben-David and D. Milstein, *Angew. Chem., Int. Ed.*, 2011, **50**, 9948–9952; (f) C. Federsel, R. Jackstell and M. Beller, *Angew. Chem., Int. Ed.*, 2010, **49**, 6254–6257; (g) M. S. Jeletic, M. T. Mock, A. M. Appel and J. C. Linehan, *J. Am. Chem. Soc.*, 2013, **135**, 11533–11536; (h) S. Moret, P. J. Dyson and G. Laurenczy, *Nat. Commun.*, 2014, **5**, 4017; (i) S. A. Burgess, A. J. Kendall, D. R. Tyler, J. C. Linehan and A. M. Appel, *ACS Catal.*, 2017, **7**, 3089–3096; (j) A. Kumar, P. Daw, N. A. E. Jalapa, G. Leitius, W. L. J. Shimon, Y. Ben-David and D. Milstein, *Dalton Trans.*, 2019, **48**, 14580–14584; (k) W. Leitner, *Angew. Chem., Int. Ed.*, 1995, **34**, 2207–2221; (l) P. G. Jessop, T. Ikariya and R. Noyori, *Chem. Rev.*, 1995, **95**, 259–270; (m) P. G. Jessop, F. Joo and C.-C. Tai, *Coord. Chem. Rev.*, 2004, **248**, 2425–2442.
- Select recent examples for forming formides: (a) Q.-Y. Bi, J.-D. Lin, Y.-M. Liu, S.-H. Xie, H.-Y. He and Y. Cao, *Chem. Commun.*, 2014, **50**, 9138–9140; (b) L. Zhang, Z. Han, X. Zhao, Z. Wang and K. Ding, *Angew. Chem., Int. Ed.*, 2015, **54**, 6186–6189; (c) A. Dubey, L. Nencini, R. R. Fayzullin,



- C. Nervi and J. R. Khusnutdinova, *ACS Catal.*, 2017, 7, 3864–3868.
- 5 Select recent examples for methanol: (a) M. Behrens, F. Studt, I. Kasatkin, S. Kuhl, M. Havecker, F. Abild-Pedersen, S. Zander, F. Girgsdies, P. Kurr, B.-L. Knief, M. Tovar, R. W. Fischer, J. K. Nørskov and R. Schlögl, *Science*, 2012, **336**, 893–897; (b) J. Graciani, K. Mudiyansele, F. Xu, A. E. Baber, J. Evans, S. D. Senanayake, D. J. Stacchiola, P. Liu, J. Hrbek, J. F. Sanz and J. A. Rodriguez, *Science*, 2014, **345**, 546–550; (c) Z. Han, L. Rong, J. Wu, L. Zhang, Z. Wang and K. Ding, *Angew. Chem., Int. Ed.*, 2012, **51**, 13041–13045; (d) N. M. Rezayee, C. A. Huff and M. S. Sanford, *J. Am. Chem. Soc.*, 2015, **137**, 1028–1031; (e) S. Wesselbaum, T. vom Stein, J. Klankermayer and W. Leitner, *Angew. Chem., Int. Ed.*, 2012, **51**, 7499–7502; (f) J. R. Khusnutdinova, J. A. Garg and D. Milstein, *ACS Catal.*, 2015, **5**, 2416–2422; (g) J. Kothandaraman, A. Goepfert, M. Czaun, G. A. Olah and G. K. Prakash, *J. Am. Chem. Soc.*, 2016, **138**, 778–781; (h) E. Balaraman, C. Gunanathan, J. Zhang, L. J. W. Shimon and D. Milstein, *Nat. Chem.*, 2011, **3**, 609–614; (i) C. A. Huff and M. S. Sanford, *J. Am. Chem. Soc.*, 2011, **133**, 18122–18125; (j) S. Wesselbaum, V. Moha, M. Meuresch, S. Brosinski, K. M. Thenert, J. Kothe, T. v. Stein, U. Englert, M. Hölcher, J. Klankermayer and W. Leitner, *Chem. Sci.*, 2015, **6**, 693–704; (k) C. M. Zall, J. C. Linehan and A. M. Appel, *J. Am. Chem. Soc.*, 2016, **138**, 9968–9977; (l) Z. Lu and T. J. Williams, *ACS Catal.*, 2016, **6**, 6670–6673; (m) A. P. C. Ribeiro, L. M. D. R. S. Martins and A. J. L. Pombeiro, *Green Chem.*, 2017, **19**, 4811–4815; (n) X. Liu, J. G. de Vries and T. Werner, *Green Chem.*, 2019, **21**, 5248–5255; (o) C. Erken, A. Kaithal, S. Sen, T. Weyhermüller, M. Hölcher, C. Werlé and W. Leitner, *Nat. Commun.*, 2018, **9**, 4521.
 - 6 Q. L. Qian, M. Cui, Z. H. He, C. Y. Wu, Q. G. Zhu, Z. F. Zhang, J. Ma, G. Y. Yang, J. J. Zhang and B. X. Han, *Chem. Sci.*, 2015, **6**, 5685–5689.
 - 7 (a) Q. Liu, L. Wu, I. Fleischer, D. Selent, R. Franke, R. Jackstell and M. Beller, *Chem-Eur. J.*, 2014, **20**, 6888–6894; (b) Y.-Y. Gui, N. Hu, X.-W. Chen, L. L. Liao, T. Ju, J.-H. Ye, Z. Zhang, J. Li and D.-G. Yu, *J. Am. Chem. Soc.*, 2017, **139**, 17011–17014; (c) Z. Zhang, L.-L. Liao, S.-S. Yan, L. Wang, Y.-Q. He, J.-H. Ye, J. Li, Y.-G. Zhi and D.-G. Yu, *Angew. Chem., Int. Ed.*, 2016, **55**, 7068–7072; (d) H. Rao, L. C. Schmidt, J. Bonin and M. Robert, *Nature*, 2017, **548**, 74–77.
 - 8 (a) J. Klankermayer and W. Leitner, *Science*, 2015, **350**, 629–630; (b) J. Klankermayer, W. Leitner, K. Beydoun and T. vom Stein, *Angew. Chem., Int. Ed.*, 2013, **52**, 9554–9557; (c) Y. Li, I. Sorribes, T. Yan, K. Junge and M. Beller, *Angew. Chem., Int. Ed.*, 2013, **52**, 12156–12160; (d) X. F. Liu, X. Y. Li, C. Qiao, H. C. Fu and L. N. He, *Angew. Chem., Int. Ed.*, 2017, **56**, 7425–7429; (e) C. Qiao, X. F. Liu, X. Liu and L. N. He, *Org. Lett.*, 2017, **19**, 1490–1493; (f) P. Daw, S. Chakraborty, G. Leitner, Y. Diskin-Posner, Y. Ben-David and D. Milstein, *ACS Catal.*, 2017, **7**, 2500–2504.
 - 9 K. Beydoun, G. Ghattas, K. Thenert, J. Klankermayer and W. Leitner, *Angew. Chem., Int. Ed.*, 2014, **53**, 11010–11014.
 - 10 Y. Li, T. Yan, K. Junge and M. Beller, *Angew. Chem., Int. Ed.*, 2014, **53**, 10476–10480.
 - 11 (a) L. Zhang, J. Cheng, T. Ohishi and Z. Hou, *Angew. Chem., Int. Ed.*, 2010, **49**, 8670–8673; (b) A. Banerjee, G. R. Dick, T. Yoshino and M. W. Kanan, *Nature*, 2016, **531**, 215–219.
 - 12 I. I. F. Boogaerts, G. C. Fortman, M. R. L. Furst, C. S. J. Cazin and S. P. Nolan, *Angew. Chem., Int. Ed.*, 2010, **49**, 8674–8677.
 - 13 Select recent examples for cyclic carbonates and polycarbonates: (a) A. M. Chapman, C. Keyworth, M. R. Kember, A. J. J. Lennox and C. K. Williams, *ACS Catal.*, 2015, **5**, 1581–1588; (b) D. J. Darensbourg and S. J. Wilson, *Green Chem.*, 2012, **14**, 2665–2671; (c) W. C. Ellis, Y. Jung, M. Mulzer, R. Di Girolamo, E. B. Lobkovsky and G. W. Coates, *Chem. Sci.*, 2014, **5**, 4004–4011; (d) C. Martin, G. Fiorani and A. W. Kleij, *ACS Catal.*, 2015, **5**, 1353–1370; (e) J. Langanke, A. Wolf, J. Hofmann, K. Böhm, M. A. Subhani, T. E. Müller, W. Leitner and C. Gurtler, *Green Chem.*, 2014, **16**, 1865–1870.
 - 14 A. Otto, T. Grube, S. Schiebahn and D. Stolten, *Energy Environ. Sci.*, 2015, **8**, 3283–3297.
 - 15 Z. Wang, X.-Y. Chen, B. Liu, Q. Liu, G. A. Solan, X.-Z. Yang and W.-H. Sun, *Catal. Sci. Technol.*, 2017, **7**, 1297–1304.
 - 16 Select recent examples for hydrogenation of esters (a) T. Zell and D. Milstein, *Acc. Chem. Res.*, 2015, **48**, 1979–1994; (b) W. Kuriyama, T. Matsumoto, O. Ogata, Y. Ino, K. Aoki, S. Tanaka, K. Ishida, T. Kobayashi, N. Sayo and T. Saito, *Org. Process Res. Dev.*, 2012, **16**, 166–177; (c) D. Spasyuk, C. Vicent and D. G. Gusev, *J. Am. Chem. Soc.*, 2015, **137**, 3743–3746; (d) K. Junge, S. Werkmeister and M. Beller, *Org. Process Res. Dev.*, 2014, **18**, 289–302; (e) S. Chakraborty, H. Dai, P. Bhattacharya, N. T. Fairweather, M. S. Gibson, J. A. Krause and H. Guan, *J. Am. Chem. Soc.*, 2014, **136**, 7869–7872.
 - 17 (a) K. Mashima, K. Kusano, N. Sate, Y. Matsumura, K. Nozaki, H. Kumobayashi, N. Sayo, Y. Hori, T. Ishizaki, S. Akutagawa and H. Takaya, *J. Org. Chem.*, 1994, **59**, 3064–3076; (b) T. Saito, T. Yokozawa, T. Ishizaki, T. Moroi, N. Sayo, T. Miura and H. Kumobayashi, *Adv. Synth. Catal.*, 2001, **343**, 264–267.
 - 18 (a) A. Pandey, C. Larroche, S. C. Ricke, C.-G. Dussap and E. Gnansounou, *Biofuels alternative feedstocks and conversion processes*, Elsevier Inc, 2011; (b) W. Chen, Y. Wang, M. Ding, S. Shi and Z. Yang, *Fuel*, 2017, **207**, 503–509; (c) M. Wierzbicki, N. Niraula, A. Yarrabothula, D. S. Layton and C. T. Trinh, *J. Biotechnol.*, 2016, **224**, 27–34.
 - 19 (a) M. Nielsen, E. Alberico, W. Baumann, H. J. Drexler, H. Junge, S. Gladiali and M. Beller, *Nature*, 2013, **495**, 85–89; (b) I. Mellone, M. Peruzzini, L. Rosi, D. Mellmann, H. Junge, M. Beller and L. Gonsalvi, *Dalton Trans.*, 2013, **42**, 2495–2501; (c) L. E. Heim, N. E. Schlörer, J.-H. Choi and M. H. G. Precht, *Nat. Commun.*, 2014, **5**; (d) Y. Musashi and S. Sakaki, *J. Am. Chem. Soc.*, 2000, **122**, 3867–3877; (e) T. J. Korstanje, J. I. van der Vlugt, C. J. Elsevier and B. de Bruin, *Science*, 2015, **350**, 298–302; (f) F. M. Geilen, B. Engendahl, M. Holscher, J. Klankermayer and W. Leitner, *J. Am. Chem. Soc.*, 2011, **133**, 14349–14358.

